Infrared Semiconductor Laser Crystallization of Silicon Thin Films Using Diamond-Like Carbon as Photoabsorption Layer

Naoki SANO, Masato MAKI[1], Nobuyuki ANDOH[1], and Toshiyuki SAMESHIMA[1]

Hightec Systems Corporation, Yokohama 222-0033, Japan
[1]*Tokyo University of Agriculture and Technology, Koganei, Tokyo 184-8588, Japan*

We report the crystallization of silicon thin films using a continuous wave (CW) infrared semiconductor laser with the assistance of diamond-like carbon (DLC) as a photoabsorption layer. A beam of a 940-nm-wavelength CW semiconductor laser was irradiated to samples of 400-nm-thick DLC/50-nm-thick Si/glass with a laser power density of $7.4–24.7\,kW/cm^2$. The beam was scanned on the samples at a speed of $15–100\,cm/s$. The DLC layer was heated to a temperature above the melting point of silicon by effective absorption of laser light. Thus, the underlying 50-nm-thick silicon films were crystallized by the heat defused from DLC. It was found that the threshold energy density for the crystallization of silicon films decreased as the laser power density increased. The maximum crystallinity factors estimated from Raman scattering spectral data of silicon films were 1 and 0.78 for laser power densities of 24.7 and $7.8\,kW/cm^2$, respectively. Electron backscattering diffraction pattern (EBSD) measurements revealed that crystalline grains were randomly oriented with an average size of $3\,\mu m$. [DOI: 10.1143/JJAP.46.1254]

KEYWORDS: polycrystalline silicon, laser crystallization, thin film transistor, diamond-like carbon, laser diode, Raman scattering, electron backscattering patterns

1. Introduction

Polycrystalline silicon films have been applied to various kinds of devices such as thin film transistors (TFTs) and solar cells. Laser crystallization processes using pulsed excimer lasers have been widely adopted for the mass production of low-temperature polycrystalline silicon (LTPS) TFTs used for switching transistors of pixels and the peripheral driver circuits of liquid crystal displays (LCDs).[1–4] However, thin silicon film has a low optical absorbance in the near-infrared region. Therefore, infrared lasers have not been used for the crystallization of silicon films. We have already proposed silicon crystallization using diamond-like carbon (DLC) films as photoabsorption layers by irradiation using a 308-nm-XeCl excimer laser[5–7] and a 1064-nm-Nd:YAG laser.[8] In recent years, there has been much interest in DLC because of its outstanding properties, such as high hardness, thermal conductivity, wear-resistance, thermal durability and chemical inertness. Therefore, it is widely utilized for technological and industrial applications such as wear resistant and protective hard coats. We paid special attention to its optical properties. It has low refractive indices from 1.3 to 1.9 and high extinction coefficients from 0.8 to 0.9 for wavelengths from 250 to 1100 nm. Therefore, laser diodes with wavelengths of 800–1000 nm can be used for the crystallization of silicon films with the assistance of DLC. The power of the continuous wave (CW) laser is very stable and easily modulated by controlling the current. In particular, infrared semiconductor lasers have a markedly high durability with a lifetime longer than 10,000 h. Now, using commercially available cheap laser diodes with an energy conversion efficiency above 40%, we can easily assemble a high power laser system whose power is much higher than that of conventional XeCl excimer lasers used for the mass production of LCD panels. If it is used for the crystallization of silicon, a large reduction of the processing time and cost of production of LCDs might be realized.[9]

In this paper, we report the dependence of the crystallinity of silicon films on the irradiation condition of the laser beam. We also discuss the change of DLC characteristics caused by the laser irradiation.

2. Experimental Details

50-nm-thick amorphous silicon (a-Si) films were formed at $300\,°C$ on glass substrates with a thickness of 0.7 mm by conventional radio-frequency (RF) plasma-enhanced chemical vapor deposition (PECVD) using mixed gases of SiH_4 and H_2. Graphitic DLC films with a thickness of 400 nm were subsequently formed on the silicon films by unbalanced magnetron sputtering (UBMS),[10] with Ar gas. Generally speaking, the hydrogen concentration in DLC formed by CVD is quite high because of the use of hydrocarbon gases, such as, C_2H_2, while DLC formed by UBMS includes no hydrogen. Therefore, no eruption with hydrogen being released occurs during laser irradiation for UBMS-DLC films. A 400-nm-thick DLC has an optical absorbance above 60% at a wavelength of 940 nm, which is expected to act as an effective absorption layer of a laser beam. On the other hand, the optical absorbance of DLC film thinner than 100 nm is lower than 20%. These are the reasons why we adopted a 400-nm-thick UBMS-DLC as a photoabsorption layer.

Figure 1 shows the experimental setup for laser irradiation with the beam scanning mechanisms. Laser irradiation normal to DLC with underlying silicon films was carried out in air using a fiber-coupled CW laser diode with a wavelength of 940 nm and a maximum power of 20 W. The diameter of the core and the numerical aperture (NA) of the fiber were $400\,\mu m$ and 0.22, respectively. The diverging beam was concentrated on the surface of DLC/Si/glass samples by a combination of six aspherical lenses for 1 : 1 image formation on samples at room temperature. The power distribution of the beam was measured using a laser beam profiler and was confirmed to have a Gaussian-like intensity profile. The size of the beam spot can be controlled by changing the working distance between the lens and the sample surface. The full width at half maximum (FWHM) of the laser power distribution was changed from $500\,\mu m$
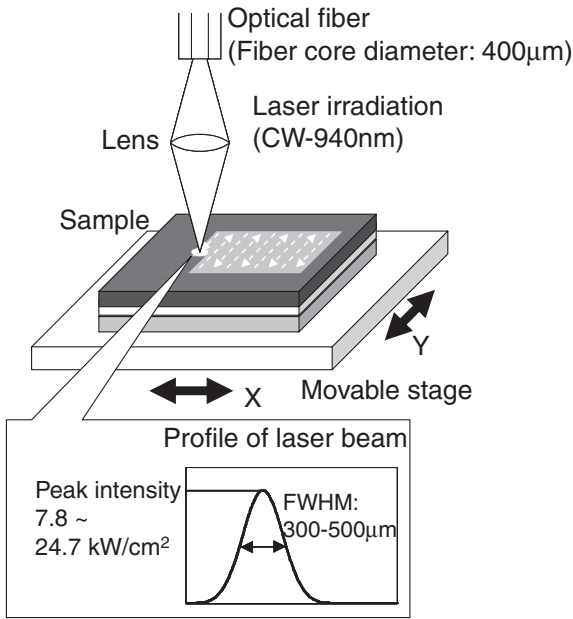
Fig. 1. Experimental setup for laser irradiation with beam scanning mechanism.

Fig. 2. Optical absorbance of 400-nm-thick DLC/50-nm-thick Si/glass at various scanning velocities of 20 W laser. Also, the absorption spectrum of the 50-nm-thick a-Si/glass is shown. The peak power density of the laser beam was 7.8 kW/cm^2.

Fig. 3. Raman scattering spectra of 400-nm-thick DLC modified by laser irradiation at scanning velocity of 15–50 cm/s with peak power density of 7.8 kW/cm^2.

(defocused) to 300 μm (focused). The peak power density was changed from 7.8 to 24.7 kW/cm^2, by varying the beam width from 500 to 300 μm at the laser power of 20 W. Samples were mounted on an *X–Y* stage driven by linear motors at a constant velocity of 15–100 cm/s in the *Y* direction keeping the size, shape, and intensity of the laser spot. The stage is also moved in the *X* direction. Using this equipment, samples with an area up to 20 × 20 cm^2 can be annealed uniformly.

Before laser irradiation, the optical absorption spectra of DLC/Si/glass samples were obtained by measuring the optical transmissivity and reflectivity spectra as a function of wavelength from 250 to 1100 nm. Raman scattering spectral measurement using a 514.5-nm-Ar-ion laser as an excitation light was also carried out in order to analyze the structural modification of DLC induced by laser irradiation. Then, the DLC films were removed using oxygen plasma at 250 °C. Raman scattering spectra were measured in order to analyze the influences of the laser irradiation condition on the crystallinity of silicon films. Electron backscattering diffraction pattern (EBSD) measurements also were carried out in order to investigate the grain structure of the crystallized silicon films.

3. Results and Discussion

Changes in the optical absorption spectra with 20 W laser irradiation at a scanning velocity of 15–50 cm/s are shown in Fig. 2, in which the peak power density and FWHM of the laser spot were 7.8 kW/cm^2 and 500 μm, respectively. It also includes the absorption spectrum for an only 50-nm-thick a-Si on glass for comparison. The absorbance at the wavelength of 940 nm was 64.8% for 400-nm-thick DLC/50-nm-thick Si/glass, while it was 2.3% for 50-nm-thick Si/glass. Although the absorbance at 940 nm slightly decreased at the scanning velocity lower than 20 cm/s, DLC effectively absorbed the 940-nm-laser energy under the present beam scanning conditions.
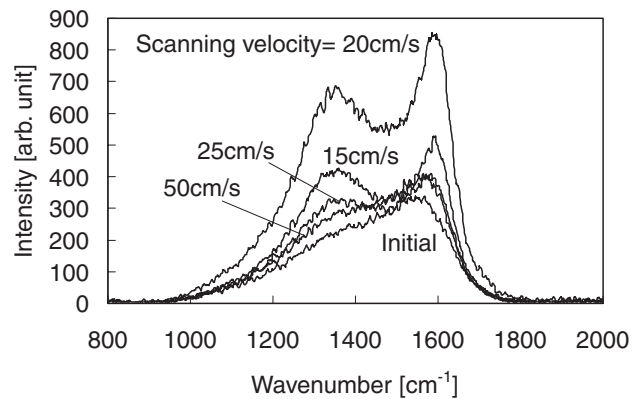
Figure 3 shows the changes in Raman scattering spectral data of DLC with laser scanning conditions. It is well known that there are two peak bands, the so-called D and G bands on the Raman spectra of DLC. The initial DLC had a D band at 1380 cm^{-1} and a G band at 1560 cm^{-1}. Spectral analyses revealed that the peak separation between the D and G bands evolved as the scanning velocity decreased. The peak wavenumber of the D band increased as the scanning velocity decreased; on the other hand, that of G band decreased as the scanning velocity decreased. The FWHM of the D band decreased from 352 cm^{-1} for no irradiation to 310 cm^{-1} at 15 cm/s and that of the G band changed from 158 to 105 cm^{-1}. Furthermore, the ratio of D band intensity *I*(D) to G band intensity *I*(G) increased from 2.66 for no irradiation to 3.20 at the scanning velocity of 15 cm/s. Both increases in the peak wavenumber and *I*(D)/*I*(G) mean an occurrence of clustering of the sp^2 phase in the atomic bonding network in DLC, which results in modification from graphite to nanocrystalline graphite.[11] These results show that DLC films were heated to a high temperature by the laser irradiation.

Figure 4 shows Raman scattering spectra of 50-nm-thick Si/glass measured after the removal of DLC for the laser irradiations at different scanning velocities. The power and
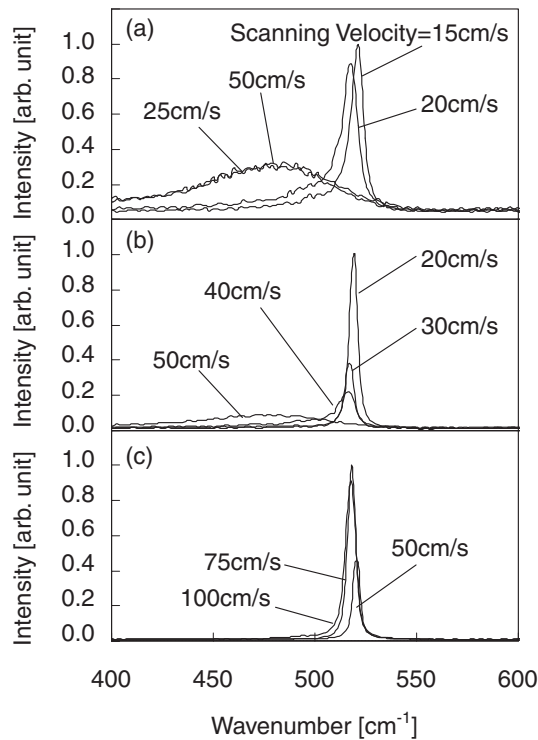
Fig. 4. Raman scattering spectra at different scanning velocities of laser beam for the 400-nm-thick DLC. The laser power densities were (a) 7.8, (b) 12.4, and (c) 24.7 kW/cm^2.

Fig. 5. Crystallinity factor of 50-nm-thick Si films as a function of scanning velocity of laser beam with peak power densities of 7.8, 12.4, and 24.7 kW/cm^2. The thickness of DLC was 400 nm.

FWHM of the laser spot were (a) 20 W, 500 μm, (b) 10 W, 300 μm, and (c) 20 W, 300 μm. The peak power densities of (a), (b), and (c) were estimated to be 7.8, 12.4, and 24.7 kW/cm^2, respectively. In Fig. 4(a), crystallization of silicon films occurred at the scanning velocity below 20 cm/s. The peak of the transverse optical (TO) phonon mode of crystalline silicon shifted from 516.2 cm^{-1} at 20 cm/s to 519.7 cm^{-1} at 15 cm/s for the 400-nm-thick DLC. Generally speaking, the peak wavenumber increases as an enlarging of the size of polycryatalline grains results in the stress relaxation of silicon films. In each case, it was found that the peak shifts to a higher value and a narrowing of peak width occurred with decreasing scanning velocity. In the case of Fig. 4(b) at the scanning velocity of 40 cm/s, silicon films were crystallized even though the laser power was just half of (a). As the peak power density for (b) was higher than that for (a), the silicon was crystallized at higher scanning velocity. In Fig. 4(c) with the highest power density of 24.7 kW/cm^2, the silicon films were crystallized even at the maximum velocity of 1 m/s. We can define the dwell time of the laser beam as (beam width)/(scanning velocity). In other words, a fixed position on the sample is continuously subjected to irradiation by one laser scanning during this dwell time. As we adopt FWHM as a typical beam width, approximately, the dwell times for crystallization are 2.5 ms for (a), 0.6 ms for (b), and below 0.3 ms for (c). Thus, the threshold energy densities for crystallization were roughly estimated to be 14.8 J/cm^2 for (a), 7.44 J/cm^2 for (b), much lower than 7.4 J/cm^2 for (c). At a long dwell time, a large amount of thermal energy is dissipated to the glass substrate with no use for crystallization, and this is the reason why rapid irradiation is necessary for crystallization with high
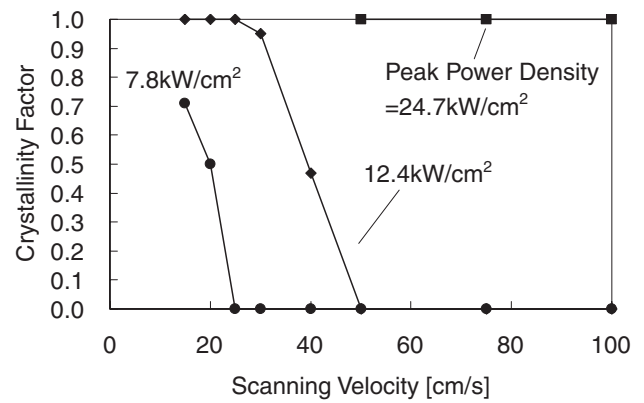
energy efficiency. To achieve more rapid irradiation, smaller beam size and higher scanning velocity will be required. A minimum FWHM of 4.5 cm^{-1} at a peak wavenumber of 518.5 cm^{-1} was observed for the power density of 24.7 kW/cm^2 and beam scanning speed of 75 cm/s, while the width of the TO phonon peak at 520.4 cm^{-1} of single-crystalline Si was 3.85 cm^{-1}.

By peak analysis, Raman spectra in Fig. 4 can be separated into phonon peaks of crystalline, nanocrystalline, and amorphous silicon components around the wavenumbers of 520, 500, and 480 cm^{-1}, respectively. We defined the crystallinity factor as the crystalline peak components to the totally integrated intensity of Raman spectra of silicon films. Figure 5 shows the crystallinity factor of the 50-nm-thick silicon films as a function of scanning velocity with different power densities of 7.8, 12.4, and 24.7 kW/cm^2. The crystallinity factor increased as the scanning velocity decreased under each condition. The maximum crystallinity factor of 0.71 was obtained at 15 cm/s for the power density of 7.8 kW/cm^2. On the other hand, in the case of the focused beam with a FWHM of 300 μm, the maximum crystallinity factor was 1 for both peak power densities of 12.4 and 24.7 kW/cm^2. This means that the silicon films were completely crystallized by the present method.

EBSD measurements were also performed in order to analyze the structure of the crystalline grains of silicon films. Figure 6 shows the inverse pole figure (a) and the inverse pole mapping image with an area of $2 \times 20\,\mu m^2$ (b) of the crystallized Si film laterally grain grown region at a scanning velocity of 75 cm/s and a peak power density of 24.7 kW/cm^2. The mapping figure did not include crystalline grains smaller than 0.1 μm because of a spatial resolution of 0.1 μm in the EBSD measurement. Almost the entire the region was occupied by crystalline grains larger than 0.1 μm. Also, a lot of grains larger than 3 μm were observed. The results obtained from the EBSD measurement coincide well with those of the above Raman spectra. Furthermore, the crystal grains were randomly oriented, although it can be seen that the crystalline growth direction was affected by the laser beam scanning direction.

4. Conclusions

Infrared semiconductor laser crystallization of thin silicon
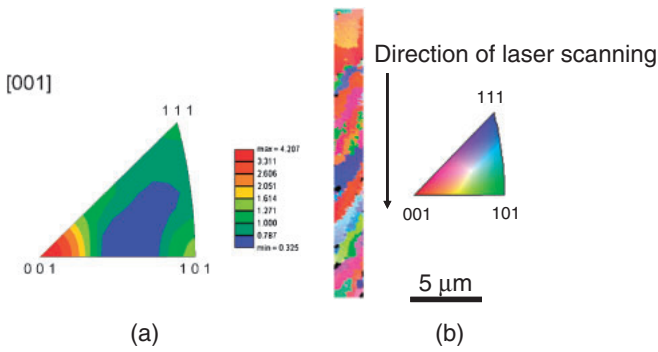
Fig. 6. Inverse pole figure (a) and mapping image of inverse pole figure (b) of 50-nm-thick Si film crystallized by laser irradiation at scanning velocity of 75 cm/s and peak power density of 24.7 kW/cm^2.

films with a heating layer of diamond-like carbon (DLC) was discussed. The structure of DLC/Si/glass had an optical absorbance above 60% for a wavelength of 940 nm. As a result of the structural modification of DLC films induced by laser irradiation with a power density of 7.8 kW/cm^2, peak separation between the D and G bands on the Raman scattering spectra developed with decreasing scanning velocity of the laser beam. This means that DLC films were heated to a high temperature.

The silicon films were crystallized well upon irradiation at a scanning velocity of 75 cm/s using a 940-nm-wavelength laser beam with a power density of 24.7 kW/cm^2. Raman scattering spectra were measured for the structural analyses of silicon films, and a sharp TO phonon peak at a wavenumber of 518.5 cm^{-1} with the minimum FWHM of 4.5 cm^{-1} was observed. This shows that silicon films were effectively crystallized using the infrared semiconductor laser. It was found that the threshold energy density for the crystallization of silicon films decreased as the laser power density increased. The maximum crystallinity factors estimated from Raman scattering spectral data of silicon films

were 1 and 0.78 for the laser power densities of 24.7 and 7.8 kW/cm^2, respectively. Electron backscattering diffraction pattern (EBSD) measurements were carried out for the analysis of the orientation and grain size of the crystallized silicon films. As a result, it appeared that the crystalline grains larger than 3 μm were randomly orientated.

The above-mentioned results showed that silicon films can be easily crystallized by infrared semiconductor laser irradiation. It might also be easy to construct a laser system with power higher than that of a conventional excimer laser using cheap infrared semiconductor laser diodes. We emphasize that it will be possible to achieve a high-throughput crystallization process for silicon films using a high-power semiconductor laser.

Acknowledgments

1) T. Sameshima, S. Usui, and M. Sekiya: IEEE Electron Device Lett. **7** (1986) 276.
2) K. Sera, F. Okumura, H. Uchida, S. Itoh, S. Kaneko, and K. Hotta: IEEE Trans. Electron Devices **36** (1989) 2868.
3) T. Serikawa, S. Shirai, A. Okamoto, and S. Suyama: Jpn. J. Appl. Phys. **28** (1989) 1871.
4) A. Kohno, T. Sameshima, N. Sano, M. Sekiya, and M. Hara: IEEE Trans. Electron Devices **42** (1995) 251.
5) T. Sameshima and N. Andoh: Mater. Res. Soc. Symp. Proc. **849** (2004) 133.
6) T. Sameshima and N. Andoh: Dig. Tech. Pap. AM-LCD 05, 2005, p. 175.
7) T. Sameshima and N. Andoh: Jpn. J. Appl. Phys. **44** (2005) 7305.
8) N. Andoh, T. Sameshima, M. Maki, and N. Sano: Proc. 2nd Int. TFT Conf. 2006, p. 142.
9) N. Sano, M. Maki, N. Andoh, and T. Sameshima: to be published in Mater. Res. Soc. Symp. Proc. (San Francisco, CA, 2006).
10) S. Yang, D. Camino, A. H. S. Jones, and D. G. Teer: Surf. Coat. Technol. **124** (2000) 110.
11) A. C. Ferrari and J. Robertson: Phys. Rev. B **61** (2000) 14095.